Journal of Fluorine Chemistry 244 (2021) 109747

Contents lists available at ScienceDirect

Journal of Fluorine Chemistry

journal homepage: www.elsevier.com/locate/fluor

Perfluoropolyether-based oleophobic additives: Influence of molecular weight distribution on wettability of polyethylene terephthalate films

Tugba Demir Caliskan [a,b,*], Liying Wei [b], Igor Luzinov [b,**]

[a] Department of Chemical Engineering, Faculty of Engineering, Ankara University, Tandogan, 06100 Ankara, Turkey
[b] Department of Materials Science and Engineering, Clemson UniverSity, Clemson, SC, 29634, United States

ARTICLE INFO

Keywords:
Oil repellency
Water repellency
Polyethylene terephthalate
Perfluoropolyether
Hydrophobicity
Oleophobicity

ABSTRACT

Fluorinated oligomeric polyester (FOP) with significantly different molecular weight distributions were synthesized for use as surface-active additives to alter the wettability of polyester films. Specifically, FOPs had different weight average molecular weight (M_W) of 5.4 and 10 kDA. The addition of FOPs in polyethylene terephthalate (PET) in different concentrations results in reducing the surface energy of PET/FOPs films. The PET/FOP film surfaces enriched with FOPs exhibited high water and oil repellency. It is found that not only concentration of FOPs in blends but also their M_W influences wettability of PET/FOP film surfaces. The highest values of water and oil repellency were obtained when we used either low concentrations of low M_W fluorinated polyesters that migrated to the surface easily, thus higher surface coverage were obtained, or high concentrations of higher $M_W$polyesters in the blends.

1. Introduction

Perfluoropolyether-based polymers (PFPEs) are considered safe materials since they contain units, such as -[CF_2CF_2]-, -$CF(CF_3)CF_2$, -CF_2-, or -$CF_2CF_2CF_2$- between the ether linkages as compared to perfluoroalkyl-based (PFA) materials (C_nF_{2n+1} with $n \geq 7$) which are recognized as persistent toxic materials [1–4]. In addition, they have attracted great research interest due to their low volatility, non-flammability, good thermal stability, high chemical resistance, and low friction coefficients [5–7]. Since PFPEs have low surface energy (18–22 mN/m), they have been attracted much attention for diverse applications, such as membranes, solar cells, optics, textiles, antifouling, and self-cleaning surfaces [8–15].

Altering the surface wettability of films is important for many applications, including antifouling, anti-fogging/corrosion, oil and water separation, self-cleaning coatings, microfluidics, and batteries [16–32]. It is well known that the orientation of fluoro carbon groups in the polymer chains and their compositions on the surface influence the surface wettability of films. The difference between the bulk and surface compositions of PFPE-blended films depends on the molecular weights and miscibility of PET an PFPE components and their surface energies. [33–36]. In addition, diffusion rate of PFPE chains to the top of the film surface is higher than PET. In general, the main reason of additive surface migration is that the components possess different surface energy [37–39]. Low surface energy materials migrate more to the surface than higher ones.

Migration of polymer chains and their surface segregation in the films also depend on the molecular weight differences of components in blends [40–45]. It is assumed that a limited number of polymer chains penetrate through the film and reach the air–polymer interface when chains are compressed in the normal direction to the surface. This restricted conformation of polymer chains at the surface decreased their conformational entropy more than bulk chains, thus, it caused a conformational entropy penalty. (Fig. 1) [40]. Briefly, conformational entropy penalty is significantly dependent on the molecular weight of the components [40]. Several studies reported that higher molecular weightcomponents in the blend experience a larger entropy penalty at the surface than do lower molecular weight components [40,46–48]. Therefore, it is better to use short macromolecules in blends to reduce surface energy of films [37,49–51]. Ralf Mason et al. synthesized fluorinated polystyrene with different M_W (5, 11, 25 and 145 kDA) and blended them with original polystyrene (PS). They obtained highest surface enrichment of fluorinated carbon groups on the film surfaces when they used fluorinated polystyrene polymers with lower M_W[37].

* Corresponding author at: Department of Chemical Engineering, Faculty of Engineering, Ankara University, Tandogan, 06100 Ankara, Turkey.
** Corresponding author.
E-mail addresses: tgbdemir@ankara.edu.tr (T. Demir Caliskan), luzinov@clemson.edu (I. Luzinov).

https://doi.org/10.1016/j.jfluchem.2021.109747
Received 24 December 2020; Received in revised form 8 February 2021; Accepted 11 February 2021
Available online 15 February 2021

Furthermore, even for polymer blended films with high surface energy, similar observations have been reported. For instance, Keiji et al. investigated the wettability of PS polymer when it was blended with either low surface energy material (high molecular weightpolystyrene (HM—PS)) or high surface energy material (low molecular weight poly (methyl methacrylate) (LM-PMMA)). They demonstrated that surfaces were fully covered with LM-PMMA even their surface energy was higher than that of HM—PS [40]. Jung et al. also obtained similar results as they blended HM—PS with low molecular weight poly(L-lactic acid) (LM-PLLA) polymers [51]. Again, LM-PLLA with higher surface energy covered all HS—PS surface. As a conclusion, molecular weight related entropy effect overcomes the effect of surface energy on migration of components [51].

To this end, we investigate the effects of the molecular weight distribution of FOPs on the wettability of PET/FOP. In a previous study, we found that FOPs with two C_4F_9- PFPE-O tails exhibited high water and oil repellency [52]. In this work, the same polymers with different weight average molecular weight (M_W)of 5.4 and 10 kDA were synthesized and blended with PET at various concentrations to reduce their wettability. The morphology and the wettability of the films were characterized using atomic force microscopy (AFM) and contact angle measurements, respectively.

2. Experimental section

2.1. Materials

For the synthesis of FOPs with different M_W(for FOP-5k $M_W = 5$ *kDa* and for FOP-10k $M_W = 10$ *kDa*), fluorinated ether alcohols such as 1H,1H,11H,11H-fluorinated-3,6,9-trioxaundecane-111-diol (PFPE-diol) and 1H,1H-fluorinated-3,6,9-trioxatridecan-1-ol (C_4F_9-PFPE−OH) were purchased from Synquest Laboratories. Isophthaloyl chloride (IsoCl), triethylamine (Et_3N) and methyl ethyl ketone (MEK) are purchased from Sigma Aldrich. All monomers are used as received. In addition,) commercial-grade PET, and its solvent 1,1,1,3,3,3-Hexafluoro-2-propanol (HFIP) were purchased from Unifi and Oakwood Products, Inc. respectively.

2.2. Synthesis of FOPs and PET/FOP film preparation

FOPs with different molecular weight distributionswere synthesized following the procedure reported elsewhere [52]. Synthesis was conducted in two steps, *(i) pre-polymerization in solution* and *(ii) melt polymerization*. Experimental details of FOPs polymerization are given in the online Supporting Information (**S1**). After synthesis of FOPs, Si wafers were dip coated from PET/FOP blends in HIPF solution. Film preparation method is also detailed in **S2.**

2.3. Characterization methods

Molecular weight distributions of FOP polymers were determined using the gel permeation chromatography (GPC, Waters, Breeze). For the GPC calibration, polystyrene standards were employed. Chemical structures of FOPs were characterized by ATR-FTIR and ^{19}F NMR using the Thermo Nicolet 6700 FTIR spectrometer and the 300 MHz Bruker Avance II NMR, respectively. In addition, a Perkin Elmer TGA was used to determine decomposition temperature (*T*d) of FOPs. Their glass transition (T_g) and melting (T_m) temperatures are obtained with using a DSC 2920 (TA Instruments). Atomic force microscopy (AFM, Digital Instruments, Inc.) was conducted to analyze the surface morphology of PET/FOP film surfaces. Contact angle measurements were performed using a drop-shape analysis instrument (DSA10, Kruss, Germany).

3. Results and discussions

It is well known that polyethylene terephthalate is generally synthesized through direct polycondensation or transesterification polymerization at high temperatures (>200 °C) to achieve high conversion [53,55]. Herein, we synthesized FOPs in two steps. First, a low-temperature (70 °C) process was carried out due to the fact that perfluoroether alcohols used in the synthesis possess low boiling points [52,55]. Later, high temperature (150–200 °C) process was performed. Finally, FOP polyesters were obtained.

According to our previous study, we found that oligomeric polyesters with lower molecular weight migrate easily to the PET film surface because of their high chain mobility. Thus, the migration of fluorinated carbon groups (-CF_2, -CF_3) to the surface results in higher oil and water repellency [52]. Moreover, FOPs with two C_4F_9-PFPE-O tails exhibited the highest hydrophobicity and oleophobicity[52]. In this study, we synthesized this best FOP again with M_W of *5.4 kDa (FOP-5k)* and *10 kDa (FOP-10k)* and blend them with PET to investigate how M_W of the FOPs influence the wettability PET/FOP surfaces. A general schematic of FOP polyester synthesis is shown in Fig. 2. We used C_4F_9-PFPE−OH in excess (Cl:OH 1:1.05) in the synthesis to terminate with C_4F_9-PFPE-O-segments on both ends of FOP polymers (Fig. 2).

The FOP synthesis procedure is detailed in **S1**. Interestingly, we obtained FOP polyesters with two different $M_W$even using the same amounts of monomers during synthesis. This was because we used different batches or stocks of monomers without purification. Thus, monomer purity was inconsistent. We claim that the level of impurity in the monomers affects the polymerization rate. Therefore, we obtained different M_W.

For the practical reasons it is important to understand how molecular weight distribution influences efficiency of low-surface energy additives. According to GPC results shown in Table 1, oligomers with M_W of 5000–10,000 g/mole and PDI of 10–11 were synthesized. It is found that the presence of ~25% of lower molecular weight oligomers in polymers results in a high PDI (as shown in **S3)**. Indeed, the presence of low molecular weightfractions causes quite asymmetric distribution in the molecular weight of FOPs (**SI**Fig. S2 and Fig. S**3**). The peak value of the distribution (indicating molecular weight for the major FOP fraction) is very close to M_W and, thus, the number average molecular weight (M_n)

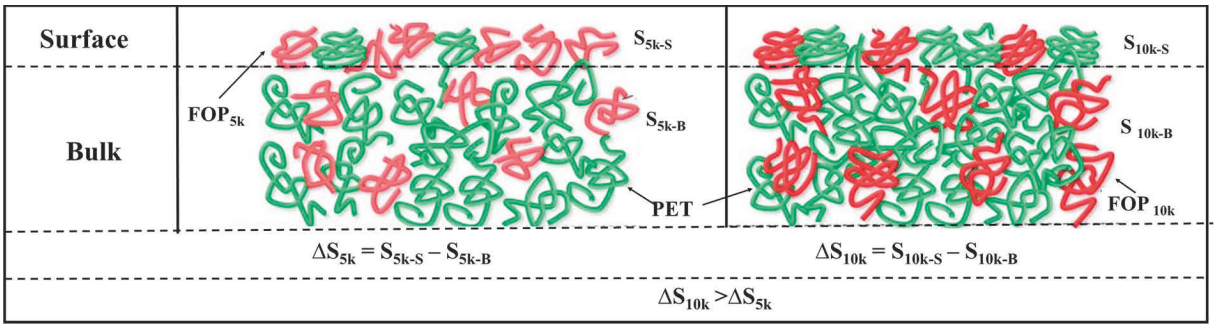

Fig. 1. Scheme of the surface arrangement of FOP-5k and FOP-10k. Their entropy changes between the surface and bulk.

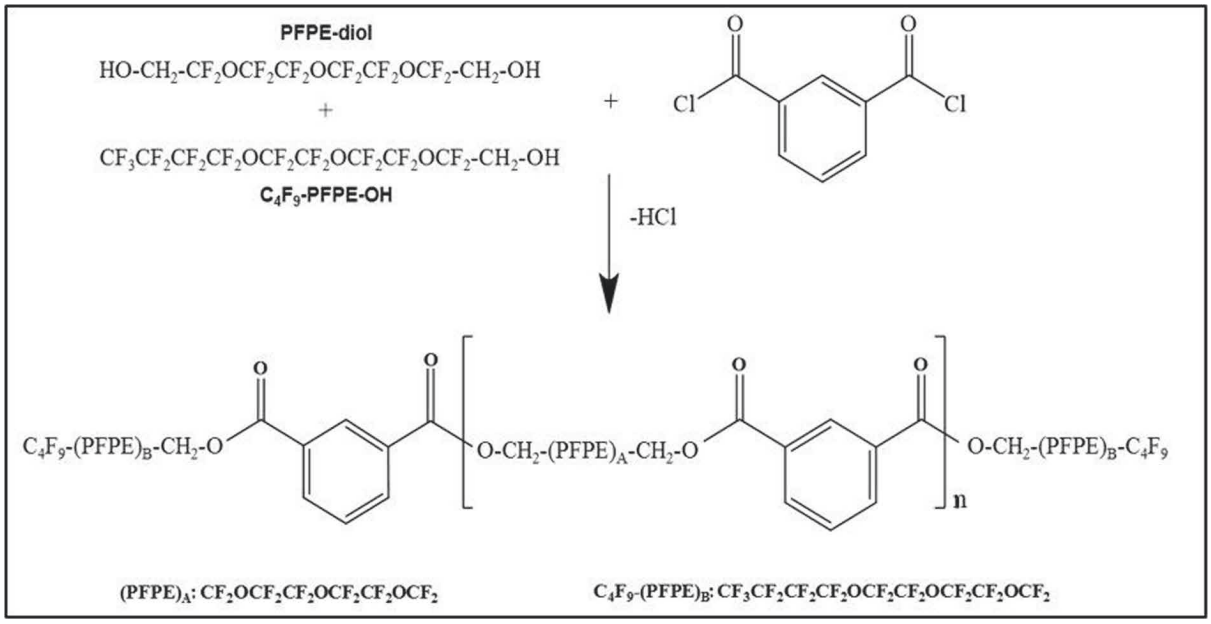

Fig. 2. General schematics for synthesis of FOP polyester.

Table 1
Major characteristics of FOPs.

FOP	M_W (g/mole)	PDI	T_g (°C)	T_m (°C)	ΔH_f (J/g)	Crystallinity (%)
FOP-5k	5438	10.4	−25	48	29.7	30.0
FOP-10k	10,000	10	−16	51	25.9	26.1

represents mostly the low molecular weight fraction. Therefore, M_W is used to determine the number of repeating polyester units. According to the chemical structure, the molecular weight of C_4F_9-PFPE-O- end-segment and a repeat unit of fluorinated polyester are 547 g/mole, and 540 g/mole, respectively. With these values, the numbers of repeating units in the FOP-5k and FOP-10k polyesters are found as ~8 and ~16, respectively. Therefore, FOP-10k contained a significantly greater number of non-fluorinated isophthalate units in its structure than did FOP-5k. The weight percentages of the repeating polyester units in the oligomeric chains were 80% and 89.1% for FOP-5k and FOP-10k, respectively. The polydispersion index (PDI) for both polymers are almost similar (Table 1)

3.1. Structural characterization of FOPs

ATR-FTIR and ^{19}F NMR experiments were carried out to identify the FOP polyesters. The results of ATR-FTIR and ^{19}F NMR were detailed in **S4** and **S5**, respectively. Spectral databases of organic compounds were used for the analysis [56]. Briefly, the spectrum of FOPs revealed −OC = O stretching and -C-O-C- stretching vibrations at 1749 cm^{-1} and 1269 cm^{-1}, respectively due to the reaction of perfluoro alcohols with isophthoyl acid chlorides (**SI** Fig. S**4**). In addition, -CF_2- and -CF_3 bands appeared at 1200–1100 cm^{-1}[57,58]. ^{19}F NMR results shows that fluorine atoms in -O-$\underline{CF_2}$−CH_2-O−CO- repeat units were detected from -77.30 ppm to -77.70 ppm ((a) peak shown in Fig. S**5** and Fig. S**6**). In addition, fluorine atoms present in the -CF_3 group, the -CF_2CF_2-group and -CF_2- group of FOP tail ($\underline{CF_3}$-$\underline{CF_2}\underline{CF_2}$-$\underline{CF_2}$-O-) appeared at -81.92 ppm (d), at -127.22 ppm (f) and -84.16 ppm (e), respectively.

3.2. Thermal transitions of FOP polyester

DSC experiments were carried out to determine thermal properties of FOPs. It is found that FOPs are semi-crystalline materials because they have both T_g and T_m. The midpoint T_g values of FOP-5k and FOP-10k range from -25 °C to−16 °C, while their T_m range from 48 °C to 51 °C (Table 1). In addition, it is found that the higher M_W *FOP*-10k polyester had higher T_g and T_m compared to the lower M_W FOP-5k polyester (Fig. S**7 in S6**). The increase of T_g and T_m with molecular weight is a well-established phenomenon [54,59–62].

DSC data was used to calculate the percentages of crystallinity of the FOPs using heat of fusion (ΔH_f) in **SI Eq. S1** (**S7**). The ΔH_f values of FOP-5kand FOP-10k were found to be 29.7 J/g and 25.9 J/g, respectively. In the previous study, the ΔH^f_{crys} values of the FOP were estimated to be 96.3 J/g [60]. Therefore, the total degrees of crystallinity of the FOPs were 26–30%.

3.3. Morphology of PET/FOP films

Atomic force microscopy was conducted to characterize the surface morphology of PET/FOP films. Figs. 3 and 4 show smooth polyester films with FOP-5k and FOP-10k contents, respectively. Dark domains of FOPs and a bright domain of PET matrix are formed due to the immiscibility of PET and FOPs components [52]. Thus, the size of dark domains increases with increasing the concentration of FOPs in blends

The average sizes of the FOP-5k and FOP-10k domains in the AFM topographical and phase images (shown in Fig. S**8** and Fig. S**9 in S8**, respectively**)** were calculated using the bearing ratio analysis (Abbott-Firestone curve). The results are summarized in Tables S**1** and **TableS2** in **S8**. The size of the fluorinated domains and the total FOP surface coverage depends on the concentration of FOP in blends. As increasing the FOP concentration, both of them are increased. When more than 40 wt.% FOP was used in PET, film surface was completely covered with FOP chains. This was expected because the X-ray photoelectron spectroscopy results of the fluorinated polyesters obtained in our previous study revealed that the –CF_2 and –CF_3 groups covered whole PET/FOPs film surfaces, even when the films had only 33 wt.% FOPs [52].

When the PET/FOP-5k and PET/FOP-10k films were annealed at different temperatures (140 °C or 250 °C), their morphologies were significantly changed (PET/FOP-5k in Fig. S**10** and PET/FOP-10k in Fig. S**11** in **S8**). Annealed pure PET samples are also used as a control sample. The PET crystal domains within pure PET and the PET/FOPs films were formed during annealing at 140 °C. On the other hand, spherulites are

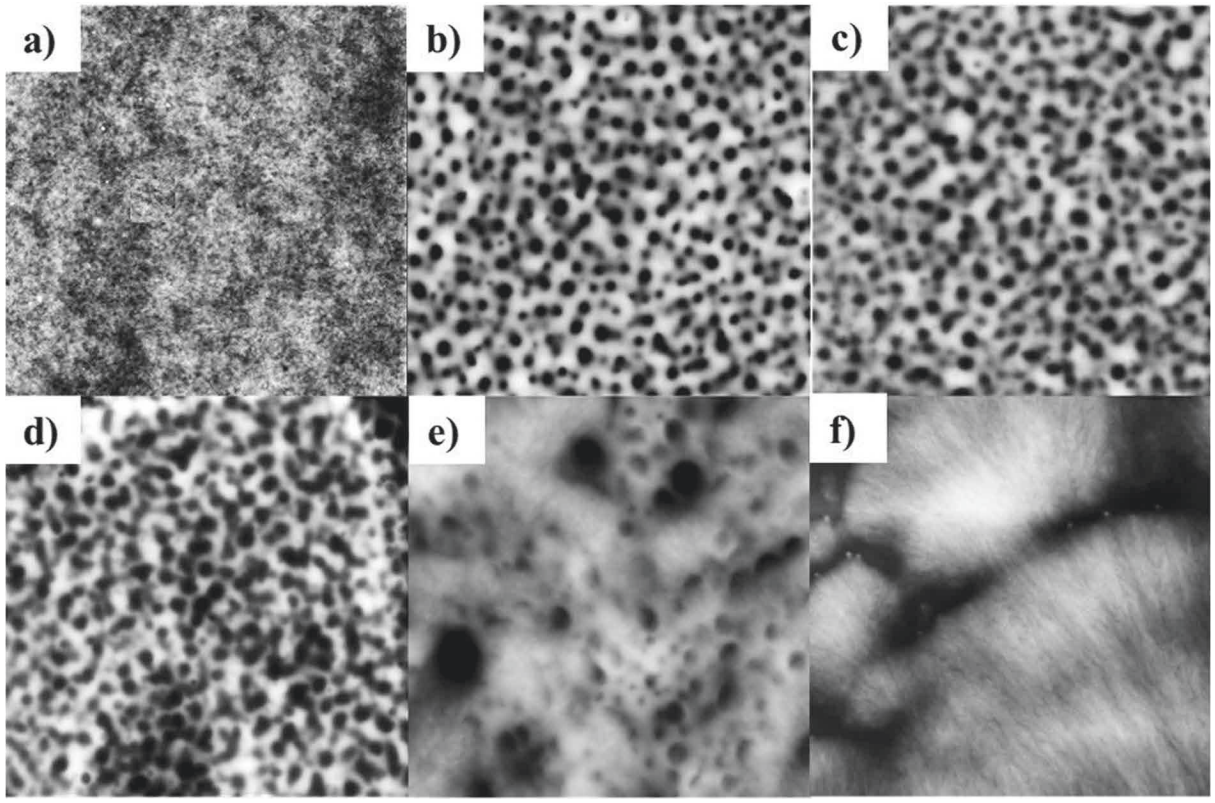

Fig. 3. AFM image of PET/ FOP-5k blended films. a) pure PET, RMS = 1 nm; b)5% FOP-5k, RMS = 25 nm; c)10% FOP-5k, RMS = 10 nm; d)20% FOP-5k, RMS = 15 nm; e)40% FOP-5k, RMS = 32 nm; f)80% FOP-5k, RMS = 33 nm.

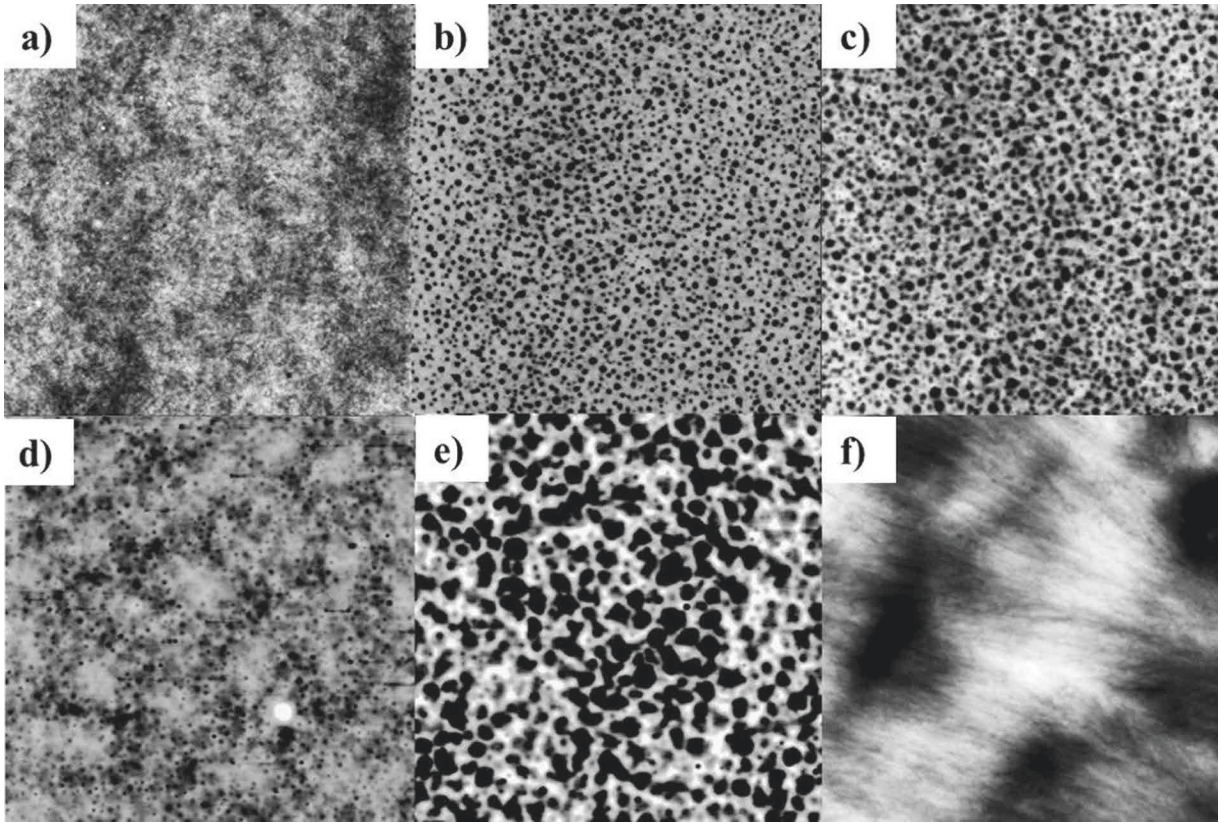

Fig. 4. AFM image of PET/FOP-10k blended films. a) pure PET, RMS = 1 nm; b);5% FOP-10k, RMS = 1 nm; c)10% FOP-10k, RMS = 2 nm; d)20% FOP-10k, RMS = 2 nm; e)40% FOP-10k RMS = 2 nm; f)80% FOP-10k, RMS = 20 nm.

obtained when films were annealed at 250 °C which is a melting temperature of PET. These structures became visible as the concentration of the fluorinated polymer increased (Fig. S**10** and Fig. S**11 (o–p,s–t) in S8**).

3.4. Surface wettability of PET/FOP films

The contact angle measurements were conducted to determine water and oil repellent properties of PET/FOPs films. The contact angle of water (WCA) and hexadecane (HCA) measurements are shown in Fig. 5. It is known that hexadecane wets PET completely (HCA < 5°), but it is patially wettable with water (WCA ≈ 58°). In our previous study, it was found that the incorporation of FOP with different end groups into the PET films significantly increased their hydrophobicity and oleophobicity [52]. The data obtained in this research confirmed the results of the previous study even when the M_W of the FOPs were altered. Again, it was found that that the addition of only 5% FOP polyester to PET increased WCA and HCA to the level of 70–80°and the level of 40–50°, respectively. Although HCA did not change significantly even as the concentration of FOP was increased up to 80%, WCA further increased to the level of 80–90°.

The effect of $M_W$on wettability of films was investigated as well. As can be seen in Fig. 6, film containing FOP-5k at low concentrations possess higher WCA than FOP-10k since short polymer chains migrate easily to through PET to enrich the surface. This was expected since short polymer chains on the surface exhibit reduced conformational entropy penalties compared to longer ones. By contrast, for high-concentration PET/FOP films, WCA increased as the M_W increased because the FOP-10k polymer exhibited higher surface enrichment of

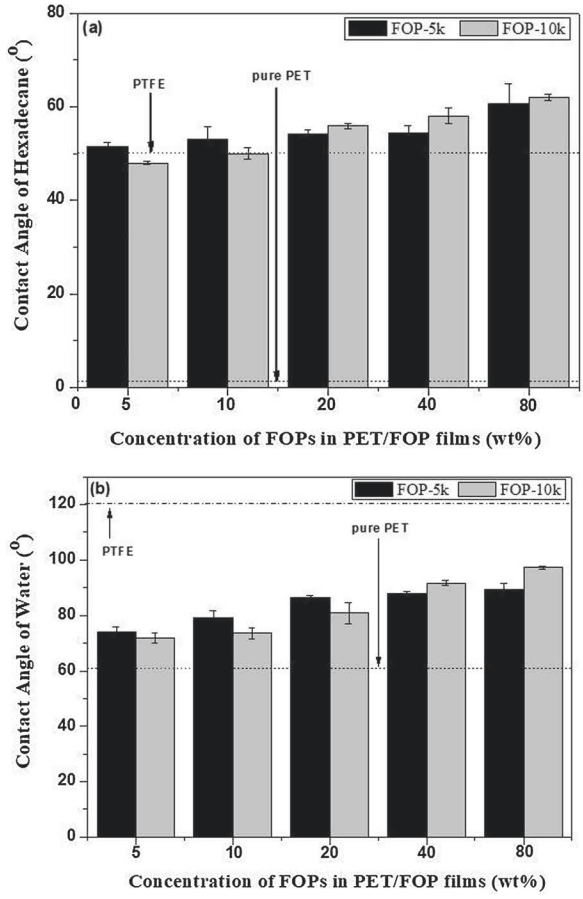

Fig. 5. Contact angle of hexadecane (a) and water (b) on PET/ FOP films. (black)PET/FOP-5k films, (gray) PET/FOP-10k films. Contact angles for PET and PTFE are given for comparison.

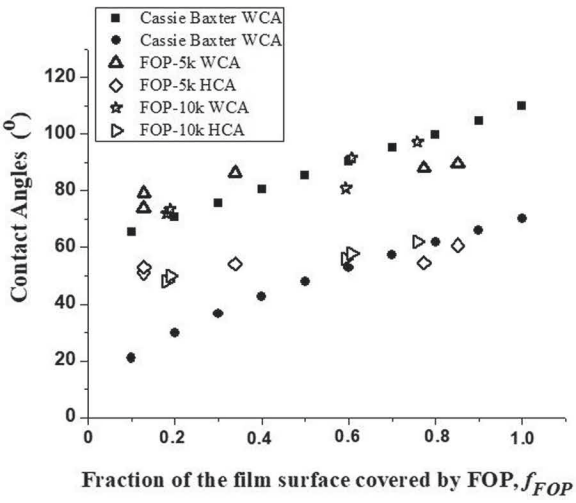

Fig. 6. WCA and HCA as predicted by the Cassie – Baxter model along with the experimentally measured contact angles for PET/FOP films. Fraction of the film covered with FOP is determined from the AFM phase images.

the $-CF_3$ groups, leading to reduce surface energy. Therefore, we conclude that end groups (-C_4F_9-PFPE-O) of FOPs dominantly affected WCA instead of their M_W when FOPs were used at high concentrations.

The Cassie–Baxter model (Eq. 1) is used for determining the effects of FOP contents in the blends on contact angles measurements. The apparent contact angle of a liquid θ_{CB} on PET/FOP surface was found using the Eq. 1[67]:

$$\cos\theta_{CB} = f_{FOP}\cos\theta_{Y-FOP} + f_{PET}\cos\theta_{Y-PET} \quad (1)$$

where θ_{CB} is the Cassie-Baxter apparent contact angle, $\theta_{Y\text{-}PET}$ and $\theta_{Y\text{-}FOP}$ are the Young contact angles of solvents on homogeneous, smooth and bare PET and FOP surfaces, respectively, and their surface area fractions are shown f_{PET} and f_{FOP}, as well

The f_{FOP} and f_{PET} of the component surfaces are obtained from AFM phase images (**SI** Table S**1** and Table S**2**). We could not measure $\theta_{Y\text{-}FOP}$ on bare FOP films since they dewet. Therefore, we assumed that the maximum CA value ($\theta_{Y\text{-}FOP}$) is the same for both fluorinated polyesters (FOP-5k and FOP-10k) as described before [52] and did calculations accordingly. The highest reported HCA and WCA values for PFPE in the literature are ~70° for and ~110°, respectively [68,69]. The apparent contact angle (θ_{CB}) of hexadecane and water for all films were calculated using the Eq. 1. The apparent contact angles with increasing the surface fractional area of FOP is illustrated in Fig. 6. The experimental data were also compared with data obtained from the model. It is found that although the measured HCA and WCA did not vary significantly with increasing the FOPs content, whereas θ_{CB} linearly increases. Specifically, HCA did not change with FOP content, but it was significantly higher than the value predicted at lower FOP concentrations.

We also studied the influence of annealing on WCA and HCA (Fig. 7). Herein, two annealing conditions, 140 °C for 3 h and 250 °C for 30 min, were employed. The former temperature (140 °C) was selected because it is higher than the T_g of both FOP polyesters and PET (70–80 °C [65, 66]) but lower than the T_m of PET (250–260 °C [65,66]). It was found that as the temperature increased, the migration of FOPs increased, leading to full coverage on PET. The comparison between the wettability of the PET/FOP-5k and PET/FOP-10k films annealed at 140 °C revealed that up to 40% FOP in blends, PET/P3–5k exhibited stronger water repellency than PET/FOP-10k. For more than 40% FOP content, PET/FOP-10k films exhibited the highest repellency. Again, conformational entropy influences the observed behavior. During annealing all chains become more mobile in the blends. However, at low concentrations, high M_W mobile polymer chains incurred large entropy penalties during migration to the surface. Therefore, surfaces are covered by low

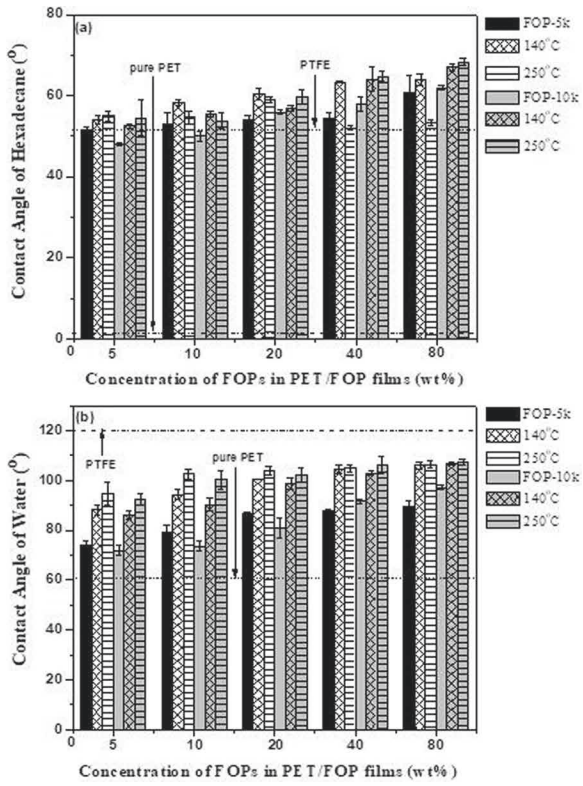

Fig. 7. Contact angle measurements. a) hexadecane and b) water contact angle on PET/ FOP films. (solid) before annealing, (mesh) after annealed films at 140°C and (line) after annealed films at 250°C. Contact angles for PET and PTFE are given for comparison.

M_W chains that decrease the surface energy of films. At high concentrations, the surfaces were enriched with FOP-10k polymers, leading to strong water repellency. In addition, the shrinkage of PET that occurred upon crystallization from the melt increases the migration of FOP chains. Moreover, the shrinkage (at 250 °C) could be more than that upon annealing at 140 °C. Therefore, at low concentrations, samples annealed at 250 °C exhibited the highest water repellency.

3.5. Surface energy of PET/FOP films

Contact angle measurements were used to calculate the surface energy (σ) of films with the Owens-Wendt method (**S8**) [73]. As shown in Fig. 8, although bare PET films have high surface energy (46 mN/m), the addition of FOPs in to PET reduced its surface energy. Even at low oligomer concentrations, significant reduction in surface energy is obtained. For only 5% FOP addition, the surface energy was 34.6 mN/m and 34.3 mN/m for FOP-5k and FOP-10k, respectively. Notably, the surface energy of PET/FOPs films with 5% additives was just 20% higher than that of Teflon™ (18.5 mN/m). In addition, the maximum reduction in surface energy was obtained when 80% FOP was loaded ($\sigma_{FOP\text{-}5k} = 22$ mN/m and $\sigma_{FOP\text{-}10k} = 18.6$ mN/m). Fig. 8shows that annealed surface possess lower surface energy than non-annealed ones. It is expected since the surfaces ere enriched with fluorinated chains Especially, at high concentrations, annealed PET/FOP surfaces had lower surface energy than PTFE.

As a comparison of the surface energy values of the PET/FOP-5k and PET/ FOP-10k films, it is found that generally the PET/FOP-10k films had higher surface energy than PET/FOP-5k films when they were used at low concentration. Specifically, among the annealed samples (140 °C), the PET/FOP-10k films had higher surface energy at all compositions than the lower M_W FOP films. This was expected because the high M_W polymer has entropy penalty compared to the FOP-5k. When the system temperature increased further, most of the FOP-5k chains migrated to the surface easily.

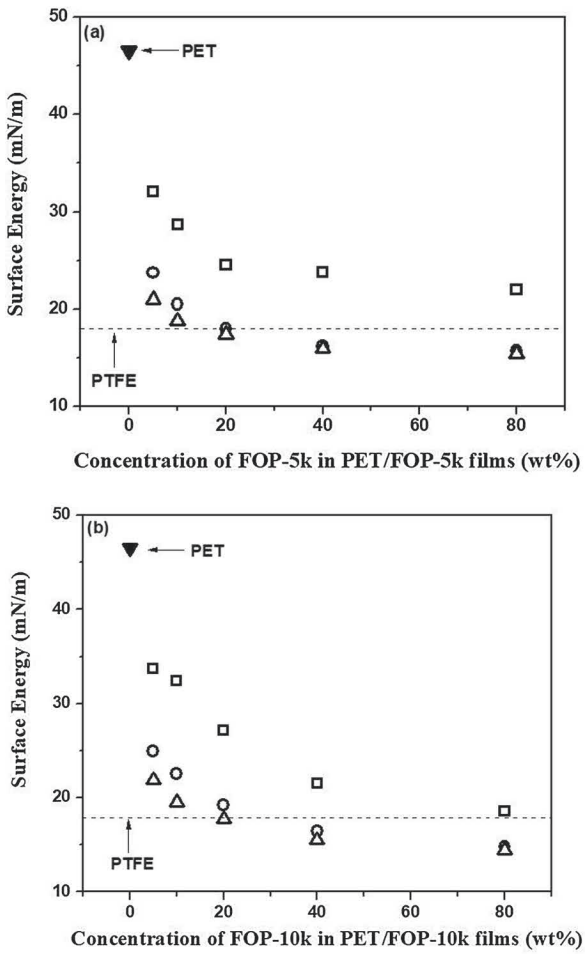

Fig. 8. Surface energy of (a) PET/FOP-5k films and (b) PET/FOP-10k films. □) before annealing, ○) after annealing at 140°C and Δ) after the annealing at 250°C. Surface energies for PET and PTFE are given for comparison.

4. Conclusion

FOP polyesters, especially the ones terminated with fluorinated carbon groups (CF_3), were employed as low-surface-energy additives in PET coatings. FOPs having two C_4F_9- PFPE-O tails with different weight average molecular weights (5.4k and 10k) were synthesized via polycondensation polymerization. When they were blended with PET films, FOPs migrated to the film surface, and reduce the surface wettability. It is found that concentration of fluorinated polyesters in the films influenced more on wettability of PET/FOP films than M_W of the fluorinated polyester. However, the highest values of water and oil repellency were obtained when we used either low concentrations of low M_W fluorinated polyesters that migrated to the surface easily, or high concentrations of higher $M_W$polyesters in the blends.

Data availability

The raw/processed data required to reproduce these findings cannot be shared at this time due to legal or ethical reasons. In addition, the data also forms part of an ongoing study.

Declaration of Competing Interest

The authors declare no conflict of interest.

Acknowledgements

The research reported was partially supported by the National Science Foundation via EPSCoR OIA-1655740 and I/UCRC-1034979. The authors gratefully acknowledge Dr. Phillip A. Brown and Dr. Alex Kitaygorodskiy of Clemson University for their help and advice.

Appendix A. Supplementary data

Supplementary material related to this article can be found, in the online version, at doi:https://doi.org/10.1016/j.jfluchem.2021.109747.

References

[1] C. Lau, K. Anitole, C. Hodes, D. Lai, A. Pfahles-Hutchens, J. Seed, Perfluoroalkyl acids: a review of monitoring and toxicological findings, Toxicol. Sci. 99 (2007) 366–394, https://doi.org/10.1093/toxsci/kfm128.

[2] M. Houde, A.O. De Silva, D.C.G. Muir, R.J. Letcher, Monitoring of perfluorinated compounds in aquatic Biota: an updated review, Environ. Sci. Technol. 45 (2011) 7962–7973, https://doi.org/10.1021/es104326w.

[3] S. Hong, J.S. Khim, T. Wang, J.E. Naile, J. Park, B.-O. Kwon, S.J. Song, J. Ryu, G. Codling, P.D. Jones, Y. Lu, J.P. Giesy, Bioaccumulation characteristics of perfluoroalkyl acids (PFAAs) in coastal organisms from the west coast of South Korea, Chemosphere 129 (2015) 157–163, https://doi.org/10.1016/j.chemosphere.2014.06.023.

[4] R.C. Buck, J. Franklin, U. Berger, J.M. Conder, I.T. Cousins, P. de Voogt, A. A. Jensen, K. Kannan, S.A. Mabury, S.P. van Leeuwen, Perfluoroalkyl and polyfluoroalkyl substances in the environment: terminology, classification, and origins, Int. Environ. Assess. Manag. 7 (2011) 513–541, https://doi.org/10.1002/ieam.258.

[5] G. Lopez, B. Ameduri, J.-P. Habas, A versatile strategy to synthesize perfluoropolyether-based thermoplastic fluoropolymers by alkyne-azide step-growth polymerization, Macromol. Rapid Commun. 37 (2016) 711–717, https://doi.org/10.1002/marc.201500658.

[6] M. Toselli, M. Messori, R. Bongiovanni, G. Malucelli, A. Priola, F. Pilati, C. Tonelli, Poly(ε-caprolactone)-poly(fluoroalkylene oxide)-poly(ε-caprolactone) block copolymers. 2. Thermal and surface properties, Polymer 42 (2001) 1771–1779, https://doi.org/10.1016/S0032-3861(00)00568-1.

[7] C.M. Friesen, B. Améduri, Outstanding telechelic perfluoropolyalkylethers and applications therefrom, Prog. Polym. Sci. 81 (2018) 238–280, https://doi.org/10.1016/j.progpolymsci.2018.01.005.

[8] G. Trusiano, A. Vitale, M. Rizzello, C. Bonneaud, C. Joly-Duhamel, C.M. Friesen, R. Bongiovanni, Controlling perfluoropolyalkylether reaarangements at the surface of photocured networks, Eur. Polym. J. 121 (2019), 109285, https://doi.org/10.1016/j.eurpolymj.2019.109285.

[9] A.J. Kessman, D.K.P. Huckaby, C.R. Snyder, S.N. Kukureka, D.R. Cairns, Tribology of water and oil repellent sol–gel coatings for optical applications, Wear 267 (2009) 614–618, https://doi.org/10.1016/j.wear.2008.12.088.

[10] A. Gugliuzza, E. Drioli, A review on membrane engineering for innovation in wearable fabrics and protective textiles, J. Membr. Sci. 446 (2013) 350–375, https://doi.org/10.1016/j.memsci.2013.07.014.

[11] U.G.M. Ekanayake, D.M.S.N. Dissanayake, N. Rathuwadu, R.K.K.G.R.G. Kumarasinghe, S.K. Rodrigo, M.M.M.G.P.G. Mantilaka, Facile fabrication of fluoror-polymer self-assembled ZnO particles mediated, durable and robust omniohobic surfaces on polyester fabrics, J. Fluorine Chem. 235 (2020) 109565.

[12] H. Cui, Y. Li, X. Zhao, X. Yin, J. Yu, B. Ding, Multilevel porous structured polyvinylidene fluoride/polyurethane fibrous membranes for ultrahigh waterproof and breathable application, Compos. Commun. 6 (2017) 63–67, https://doi.org/10.1016/j.coco.2017.10.002.

[13] K. Fukada, S. Nishizawa, S. Shiratori, Antifouling property of highly oleophobic substrates for solar cell surfaces, J. Appl. Phys. 115 (2014) 103516, https://doi.org/10.1063/1.4868316.

[14] Z. Ye, Y. Chen, X. Yang, W. Hu, H. Ye, Development of perfluoropolyether modified raspberry paticles with fine hierarchical structure and their application in superhydrophobic surface, Colloids Surf. A 514 (2017) 251–259, https://doi.org/10.1016/j.colsurfa.2016.11.063.

[15] G. Trusiano, M. Rizzello, A. Vitale, J. Burgess, C.M. Friesen, C. Joly-Duhamel, R. Bongiovanni, Modification of photocurable epoxides by new perfluoropolyalkylether alcohols for obtaining self-cleaning coatings, Prog. Org. Coat. 132 (2019) 257–263, https://doi.org/10.1016/j.porgcoat.2019.02.043.

[16] S. Nishimoto, B. Bhushan, Bioinspired self-cleaning surfaces with superhydrophobicity, superoleophobicity, and superhydrophilicity, RSC Adv. 3 (2013) 671–690, https://doi.org/10.1039/C2RA21260A.

[17] K. Liu, L. Jiang, Bio-inspired self-cleaning surfaces, Annu. Rev. Mater. Res. 42 (2012) 231–263, https://doi.org/10.1146/annurev-matsci-070511-155046.

[18] X. He, P. Cao, F. Tian, X. Bai, C. Yuan, Infused configurations induced by structures influence stability and antifouling performance of biomimetic lubricant-infused surface, Surf. Coat. Technol. 358 (2019) 159–166, https://doi.org/10.1016/j.surfcoat.2018.11.035.

[19] X. Han, J. Wu, X. Zhang, J. Shi, J. Wei, Y. Yang, B. Wu, Y. Feng, Special issue on advanced corrosion-resistance materials and emerging applications. The progress on antifoling organic coating: from biocide to biomimetic surface, J. Mater. Sci. Technol. 61 (2020) 46–62, https://doi.org/10.1016/j.jmst.2020.07.002.

[20] Y. He, X. Chen, F. Dai, R. Xu, N. Yang, X. Feng, Y. Zhao, L. Chen, Immobilization of poly (N-acryloyl morpholine) via hydrogen-bonded interactions for improved separation and antifouling properties of poly(vinylidene fluoride) membranes, React. Func. Polym. 123 (2018), https://doi.org/10.1016/j.reactfunctpolym.2017.12.014.

[21] Y. Wang, D.E. Betts, J.A. Finlay, L. Brewer, M.E. Callow, J.A. Callow, D.E. Wendt, J. M. DeSimone, Photocurable amphiphilic Perfluoropolyether/Poly(ethylene glycol) networks for fouling-release coatings, Macromolecules 44 (2011) 878–885, https://doi.org/10.1021/ma102271t.

[22] Y. Xu, M. Liu, Soiling and corrosion behaviors on fluorinated anodized TiO_2 surface infused by perfluoropolyether, Surf. Coat. Technol. 307 (2016) 332–344, https://doi.org/10.1016/j.surfcoat.2016.08.091.

[23] Y. Qin, Y. Li, D. Zhang, N. Xu, X. Zhu, Wettability, durability and corrosion properties of slippery laser-textured aluminum alloy surface under water impact, Surf. Coat. Technol. 394 (2020) 125856, https://doi.org/10.1016/j.surfcoat.2020.125856.

[24] R. Bongiovanni, A. Nelson, A. Vitale, E. Bernardi, Ultra-thin films based on random copolymers containing perfluoropolyether side chains, Thin Solid Films 520 (2012) 5627–5632, https://doi.org/10.1016/j.tsf.2012.04.021.

[25] D. Devaux, I. Villaluenga, M. Bhatt, D. Shah, X.C. Chen, J.L. Thelen, J. M. DeSimone, N.P. Balsara, Crosslinked perfluoropolyether solid electrolytes for lithium ion transport, Solid State Ion. 310 (2017) 71–80, https://doi.org/10.1016/j.ssi.2017.08.007.

[26] X. Gao, X. Yan, X. Yao, L. Xu, K. Zhang, J. Zhang, B. Yang, L. Jiang, The dry-style antifogging properties of mosquito compound eyes and artificial analogues prepared by Soft lithography, Adva. Mater. 19 (2007) 2213–2217, https://doi.org/10.1002/adma.200601946.

[27] M. Nosonovsky, V. Hejazi, Why superhydrophobic surfaces are not always icephobic, ACS Nano 6 (2012) 8488–8491, https://doi.org/10.1021/nn302138r.

[28] J. Lv, Y. Song, L. Jiang, J. Wang, Bio-inspired strategies for anti-icing, ACS Nano 8 (2014) 3152–3169, https://doi.org/10.1021/nn406522n.

[29] J. Yong, Y. Fang, F. Chen, J. Huo, Q. Yang, H. Bian, G. Du, X. Hou, Femtosecond laser ablated durable superhydrophobic PTFE films with micro-through-holes for oil/water separation: separating oil from water and corrosive solutions, Appl. Surf. Sci. 389 (2016) 1148–1155, https://doi.org/10.1016/j.apsusc.2016.07.075.

[30] L. Zhang, Y. Zhong, D. Cha, P. Wang, A self-cleaning underwater superoleophobic mesh for oil-water separation, Sci. Rep. 3 (2013) 2326, https://doi.org/10.1038/srep02326.

[31] G. Zhang, M. Li, B. Zhang, Y. Huang, Z. Su, A switchable mesh for on-demand oil–water separation, J. Mater. Chem. A 2 (2014) 15284–15287, https://doi.org/10.1039/C4TA03034F.

[32] E.F. Hare, E.G. Shafrin, W.A. Zisman, Properties of films of adsorbed fluorinated acids, J. Phys. Chem. 58 (1954) 236–239, https://doi.org/10.1021/j150513a011.

[33] A. Opdahl, R.A. Phillips, G.A. Somorjai, Effect of bulk miscibility on the surface composition of Polypropylene/Poly(ethylene-co-propylene) blends, Macromolecules 35 (2002) 4387–4396, https://doi.org/10.1021/ma011773q.

[34] K. Artyushkova, J.E. Fulghum, Quantification of PVC–PMMA polymer blend compositions by XPS in the presence of x-ray degradation effects, Surf. Interface Anal. 31 (2001) 352–361, https://doi.org/10.1002/sia.953.

[35] S. Affrossman, T. Kiff, S.A. O'Neill, R.A. Pethrick, R.W. Richards, Topography and surface composition of thin films of blends of poly(methyl methacrylate) and poly (ethylene oxide), Macromolecules 32 (1999) 2721–2730, https://doi.org/10.1021/ma980804n.

[36] A. Quinn, E. Tjipto, A. Yu, T.R. Gengenbach, F. Caruso, Polyelectrolyte blend multilayer films: surface morphology, wettability, and protein adsorption characteristics, Langmuir 23 (2007) 4944–4949, https://doi.org/10.1021/la0634746.

[37] R. Mason, C.A. Jalbert, P.A.V. O'Rourke Muisener, J.T. Koberstein, J.F. Elman, T. E. Long, B.Z. Gunesin, Surface energy and surface composition of end-fluorinated polystyrene, Adv. Colloid Interface Sci. 94 (2001) 1–19, https://doi.org/10.1016/S0001-8686(01)00051-3.

[38] T. Kajiyama, K. Tanaka, A. Takahara, Surface segregation of the higher surface free energy component in symmetric polymer blend films, Macromolecules 31 (1998) 3746–3749, https://doi.org/10.1021/ma971247s.

[39] A. Budkowski, J. Klein, U. Steiner, L.J. Fetters, Diblock copolymers attached to homopolymer surfaces and interfaces, Macromolecules 26 (1993) 2470–2478, https://doi.org/10.1021/ma00062a012.

[40] K. Tanaka, A. Takahara, T. Kajiyama, Surface molecular aggregation structure and surface molecular motions of high-molecular-Weight Polystyrene/Low-Molecular-Weight poly(methyl methacrylate) blend films, Macromolecules 31 (1998) 863–869, https://doi.org/10.1021/ma9709866.

[41] M.J. Hill, P.J. Barham, A. Keller, C.C.A. Rosney, Phase segregation in melts of blends of linear and branched polyethylene, Polymer 32 (1991) 1384–1393, https://doi.org/10.1016/0032-3861(91)90418-I.

[42] M.J. Hill, P.J. Barham, A. Keller, Phase segregation in blends of linear with branched polyethylene: the effect of varying the molecular weight of the linear polymer, Polymer 33 (1992) 2530–2541, https://doi.org/10.1016/0032-3861(92)91134-N.

[43] K.H. Dai, E.J. Kramer, K.R. Shull, Interfacial segregation in two-phase polymer blends with diblock copolymer additives: the effect of homopolymer molecular weight, Macromolecules 25 (1992) 220–225, https://doi.org/10.1021/ma00027a037.

[44] R. Bongiovanni, A. Di Meo, A. Pollicino, A. Priola, C. Tonelli, New perfluoropolyether urethane methacrylates as surface modifiers: effect of

molecular weight and end group structure, React. Funct. Polym. 68 (2008) 189–200, https://doi.org/10.1016/j.reactfunctpolym.2007.09.009.
[45] E.L.S.A. Mounir, A. Takahara, T. Kajiyama, Effect of chain end group–Substrate interaction on surface molecular motion of polystyrene ultrathin films, Polym. J. 31 (1999) 550, https://doi.org/10.1295/polymj.31.550.
[46] O.N. Tretinnikov, K. Ohta, Surface segregation in stereochemically asymmetric polymer blends, Langmuir 14 (1998) 915–920, https://doi.org/10.1021/la9708391.
[47] C. Jalbert, J.T. Koberstein, I. Yilgor, P. Gallagher, V. Krukonis, Molecular weight dependence and end-group effects on the surface tension of poly (dimethylsiloxane), Macromolecules 26 (1993) 3069–3074, https://doi.org/10.1021/ma00064a012.
[48] L.A. Miccio, R. Liaño, W.H. Schreiner, P.E. Montemartini, P.A. Oyanguren, Partially fluorinated polymer networks: surface and tribological properties, Polymer 51 (2010) 6219–6226, https://doi.org/10.1016/j.polymer.2010.10.036.
[49] D.R. Iyengar, S.M. Perutz, C.-A. Dai, C.K. Ober, E.J. Kramer, Surface segregation studies of fluorine-containing diblock copolymers, Macromolecules 29 (1996) 1229–1234, https://doi.org/10.1021/ma950544z.
[50] W.W.Y. Lau, C.M. Burns, Effect of temperature and molecular weight on the rate of spreading of polystyrene melts on plane soda lime glass surfaces, J. Polym. Sci. 12 (1974) 431–439, https://doi.org/10.1002/pol.1974.180120215.
[51] J.Y. Lim, J.C. Hansen, C.A. Siedlecki, R.W. Hengstebeck, J. Cheng, N. Winograd, H. J. Donahue, Osteoblast adhesion on poly(l-lactic acid)/Polystyrene demixed thin film blends: effect of Nanotopography, surface chemistry, and wettability, Biomacromolecules 6 (2005) 3319–3327, https://doi.org/10.1021/bm0503423.
[52] T. Demir, L. Wei, N. Nitta, G. Yushin, P.J. Brown, I. Luzinov, Toward a long-chain perfluoroalkyl replacement: water and oil repellency of polyethylene terephthalate (PET) films modified with perfluoropolyether-based polyesters, ACS Appl. Mater. Interf. 9 (2017) 24318–24330, https://doi.org/10.1021/acsami.7b05799.
[53] G.G. Odian, Principles of Polymerization, Wiley-Interscience, Hoboken, NJ, 2004.
[54] J.R. Fried, Polymer Science and Technology, 3rd ed., Prentice Hall, Upper Saddle River, NJ, 2014.
[55] L. Wei, T. Demir, A. Grant, V. Tsukruk, P.J. Brown, I. Luzinov, Attainment of water and oil repellency for engineering thermoplastics without long-chain perfluoroalkyls: perfluoropolyether-based triblock polyester additives, Langmuir 34 (2018) 12934–12946, https://doi.org/10.1021/acs.langmuir.8b02628.
[56] P.B. Martin Badertscher, Erno Pretsch, Structure Determination of Organic Compounds. Tables of Spectral Data, Springer, 2009.
[57] L. Hao, Q. An, W. Xu, L. Huang, Synthesis, film morphology and hydrophobicity of novel fluorinated polyacrylate emulsion and solution on silicon wafer, Colloids Surf. A 396 (2012) 83–89, https://doi.org/10.1016/j.colsurfa.2011.12.045.
[58] T.E. Karis, B. Marchon, D.A. Hopper, R.L. Siemens, Perfluoropolyether characterization by nuclear magnetic resonance spectroscopy and gel permeation chromatography, J. Fluorine Chem. 118 (2002) 81–94, https://doi.org/10.1016/S0022-1139(02)00197-5.
[59] L.H. Sperling, Introduction to Physical Polymer Science, John Wiley & Sons, 2006.
[60] T.G. Fox, P.J. Flory, Second-order transition temperatures and related properties of polystyrene. I. Influence of molecular weight, J. Appl. Phys. 21 (1950) 581–591, https://doi.org/10.1063/1.1699711.
[61] T.G. Fox, P.J. Flory, The glass temperature and related properties of polystyrene. Influence of molecular weight, J. Polym. Sci. 14 (1954) 315–319, https://doi.org/10.1002/pol.1954.120147514.
[62] A. Keller, M. Hikosaka, S. Rastogi, A. Toda, P.J. Barham, G. Goldbeck-Wood, An approach to the formation and growth of new phases with application to polymer crystallization: effect of finite size, metastability, and Ostwald's rule of stages, J. Mat. Sci. 29 (1994) 2579–2604, https://doi.org/10.1007/BF00356806.
[65] J.R. Fried, Polymer Science and Technology, third edition, Pearson Education, 2014.
[66] G.P. Karayannidis, I.D. Sideridou, D.N. Zamboulis, D.N. Bikiaris, A.J. Sakalis, Thermal behavior and tensile properties of poly(ethylene terephthalate-co-ethylene isophthalate), J. Appl Polym. 78 (2000) 200–207, https://doi.org/10.1002/1097-4628(20001003)78:1<200::AID-APP240> 3.0.CO;2-R.
[67] A.B.D. Cassie, S. Baxter, Wettability of porous surfaces, Trans. Faraday Soc. 40 (1944) 546–551, https://doi.org/10.1039/TF9444000546.
[68] A. Vaidya, M.K. Chaudhury, Synthesis and surface properties of environmentally responsive segmented polyurethanes, J. Colloid Interface Sci. 249 (2002) 235–245, https://doi.org/10.1006/jcis.2002.8262.
[69] E. Fabbri, P. Fabbri, M. Messori, F. Pilati, C. Tonelli, M. Toselli, Surface modification of unsaturated polyester resins with perfluoropolyethers, Polimeri 795 (2004) 11–12, https://doi.org/10.14314/polimery.2004.785.
[73] D.K. Owens, R.C. Wendt, Estimation of the surface free energy of polymers, J. Appl. Polym. 13 (1969) 1741–1747, https://doi.org/10.1002/app.1969.070130815.